Very weak electron-phonon coupling and strong strain coupling in manganites

S. Cox,[1,2] J. C. Loudon,[2] A. J. Williams,[3] J. P. Attfield,[3] J. Singleton,[1] P. A. Midgley,[2] and N. D. Mathur[2]
[1]*National High Magnetic Field Laboratory, Ms-E536, Los Alamos National Laboratory, Los Alamos, New Mexico 87545, USA*
[2]*Department of Materials Science and Metallurgy, University of Cambridge, Cambridge CB2 3QZ, United Kingdom*
[3]*Centre for Science at Extreme Conditions, University of Edinburgh, Edinburgh EH9 3JZ, United Kingdom*
(Received 29 November 2007; published 28 July 2008)

We describe transmission electron microscopy experiments that demonstrate the validity of the charge density wave (CDW) Landau theory in describing the so-called stripe phase of the manganites and that permit quantitative estimates of some of the theoretical parameters that describe this state. In polycrystalline $Pr_{0.48}Ca_{0.52}MnO_3$ a lock-in to $q/a^*=0.5$ in a sample with $x>0.5$ has been observed. Such a lock-in has been predicted as a key part of the Landau CDW theory of the stripe phase. Thus it is possible to constrain the size of the electron-phonon coupling in the CDW Landau theory to between 0.08% and 0.50% of the electron-electron coupling term. In the thin film samples, films of the same thickness grown on two different substrates exhibited different wave vectors. The different strains present in the films on the two substrates can be related to the wave vector observed via Landau theory. It is demonstrated that the elastic term, which favors an incommensurate modulation, has a similar size to the coupling between the strain and the wave vector, meaning that the coupling of strain to the superstructure is unexpectedly strong.

DOI: 10.1103/PhysRevB.78.035129 PACS number(s): 71.38.−k, 75.47.Lx, 71.45.Lr

I. INTRODUCTION

The properties of the manganites comprise a zoo of delicately balanced phases in which changes in temperature, magnetic field, chemical composition, and strain (among other parameters) yield a rich tapestry of phase coexistence.[1,2] The stripe phase, which forms at low temperatures on the insulating (resistivity decreases with increasing temperature) side of the manganite phase diagram, was long thought to be driven by strong electron-phonon coupling,[3,4] since the materials are insulating at all temperatures. However, recent experimental work has led to the conclusion that the stripe phase is actually a charge density wave (CDW) subject to a high level of disorder.[5] The CDW model of the stripe phase was described theoretically using a Landau theory, which successfully reproduced the observed variation of the wave vector q with composition[6] ($q/a^*=1-x$), where a^* is the reciprocal lattice vector. This theory made the prediction that for x slightly greater than 0.5, there should be a lock-in of the wave vector to $q/a^*=0.5$, though no such lock-in had ever been observed. Measurements of the wave vector of manganites with $x\geq 0.5$ always found $q/a^*\leq 1-x$.[3,7–10] Here we report an observation of such a lock-in, in $Pr_{0.48}Ca_{0.52}MnO_3$. In addition, the values of the wave vector that we observe can be used to constrain the Landau theory parameter for the electron-phonon coupling relative to the electron-electron coupling to the range 0.08%–0.50%, suggesting that the electron-phonon coupling in the manganites is extremely weak. This supports the model of a prototypical CDW, which is only weakly tied to the lattice, for the manganite stripe phase.

Landau theory also predicts[11,12] that it should be possible to tune the low-temperature superstructure of the manganites by altering the strain in a small area of a thin film. Thus far it has not been possible to measure the changes in strain,[8] and so it has not been possible to quantitatively link such changes in property to theoretical work. Here we measure the properties of the low-temperature superstructure in different known strain states using thin films of $La_{0.50}Ca_{0.50}MnO_3$, and provide a quantitative analysis of the results, allowing us to compare the size of the strain coupling and electron-electron coupling via the Landau theory.

For the thin-film experiments, the composition $La_{0.50}Ca_{0.50}MnO_3$ was chosen since it has been well characterized in both thin film[8] and polycrystalline forms. Previous work on $La_{0.50}Ca_{0.50}MnO_3$ found a q/a^* of around 0.48,[8] whereas in $Pr_{0.5}Ca_{0.5}MnO_3$, q/a^* is around 0.45.[9] In polycrystalline $La_{0.50}Ca_{0.50}MnO_3$, q/a^* exhibits values between 0.46 and 0.50 at 90 K (the intergranular variation is up to 9%; the intragranular variation is less than 1%).[3,7,13] Below the Néel transition temperature $T_N\simeq 135$ K (on cooling),[13] the positions of the superstructure reflections appear to stabilize, and it is assumed that in the absence of extrinsic factors, q/a^* would take the value 0.5. The superstructure persists up to the Curie temperature of $T_C\simeq 220$ K, and for $T_N<T<T_C$, q/a^* is hysteretic and incommensurate.[13]

Polycrystalline $La_{0.48}Ca_{0.52}MnO_3$ shows similar behavior to $La_{0.50}Ca_{0.50}MnO_3$, except that q/a^* does not lock in to 0.5 in any grains (low-temperature values lie between 0.43 and 0.475), and the variation of q/a^* with temperature does not show a hysteresis loop.[7] The compound $Pr_{0.48}Ca_{0.52}MnO_3$ was investigated here because it is predicted to have stronger electron-phonon coupling than $La_{0.48}Ca_{0.52}MnO_3$, since the Pr ion is smaller than the La ion. Stronger electron-phonon coupling should be associated with a stronger bias toward the stripe phase as opposed to the ferromagnetic (FM) phase. This is because $q/a^*=0.5$ is always observed if the stripe phase exists below $x=0.5$;[14,15] stronger electron-phonon coupling means a larger energy gain when the superstructure locks into the lattice. This effect can be observed in the phase diagrams for the two materials, in which the $Pr_{1-x}Ca_xMnO_3$ stripe-phase region extends down to $x=0.3$, whereas for $La_{1-x}Ca_xMnO_3$ it extends only to $x=0.5$.[14–16] Thus it should be more energetically favorable for the superstructure to lock

into the lattice in $Pr_{0.48}Ca_{0.52}MnO_3$ than in $La_{0.48}Ca_{0.52}MnO_3$.

It is also important to consider the effect of the oxygen stoichiometry on the stripe-phase wave vector. Samples annealed in conditions expected to give lower oxygen doping are found to lock in to $q/a^*=1-x$, whereas samples expected to have higher oxygen doping exhibit $q/a^*<1-x$ (for various $x=0.5$ samples).[10] However, there is no method of measuring oxygen stoichiometry with sufficient accuracy to detect the variation between samples. Here we use polycrystalline samples prepared under the same conditions as samples used another extensive study,[7] giving us a high degree of confidence that the grain to grain variation in oxygen stoichiometry should be the same as in the other samples, and the results should therefore be comparable. In particular, this allows us to determine that the lock-in observed in $Pr_{0.48}Ca_{0.52}MnO_3$ is unlikely to be due to variations in the oxygen stoichiometry, since if it was, a similar lock-in should have been observed during the extensive measurements of $La_{0.48}Ca_{0.52}MnO_3$.[7] In addition, all thin films are grown under the same conditions to control the oxygen stoichiometry to as great a degree as possible.

The paper is organized as follows: Sec. II gives a description of the sample preparation and experimental setup and Sec. III describes the results of the experiments on thin film $La_{0.50}Ca_{0.50}MnO_3$ and polycrystalline $Pr_{0.48}Ca_{0.52}MnO_3$, while Sec. IV discusses these results in the context of the Landau theory for manganites. A summary is given in Sec. V.

II. EXPERIMENTAL DETAILS

Films were grown by pulsed laser deposition on $NdGaO_3$ and $SrTiO_3$ substrates.[8] Three films were grown on $NdGaO_3$, with thicknesses of 44 ± 2 nm, 80 ± 3 nm, and 123 ± 3 nm as measured by high resolution x-ray diffraction. One film of thickness 44 ± 2 nm was grown on $SrTiO_3$. The 44 nm thickness is sufficiently low to preserve cube-on-cube epitaxy. Magnetization was measured using a vibrating sample magnetometer, with measurements being made for the films of 44 nm, 80 nm, and 123 nm grown on $NdGaO_3$, and a bare substrate. The measurements for the films were obtained by subtracting the substrate measurement from the thin-film measurement, after correcting for the different volumes. The polycrystalline sample of $Pr_{0.48}Ca_{0.52}MnO_3$ was prepared as described in Ref. 17. The macroscopic stoichiometry of the samples was assessed by measuring the oxygen content using iodometric titration,[18] which found the oxygen stoichiometry to be the desired value within experimental error (0.1%), and using energy dispersive x-ray analysis,[7] which found the La/Ca ratio to be at the predicted level within the error of the measurements (2%).

All the samples were prepared for transmission electron microscopy by conventional grinding and dimpling, and were thinned to electron transparency ($\sim$100 nm) by argon ion milling. Measurements were taken in a Philips CM30 transmission electron microscope (TEM) with a 90 K liquid nitrogen stage. Each diffraction pattern was taken over a time scale of seconds. Conventional imaging of the polycrystalline sample indicated that the grain size was ~2 μm.

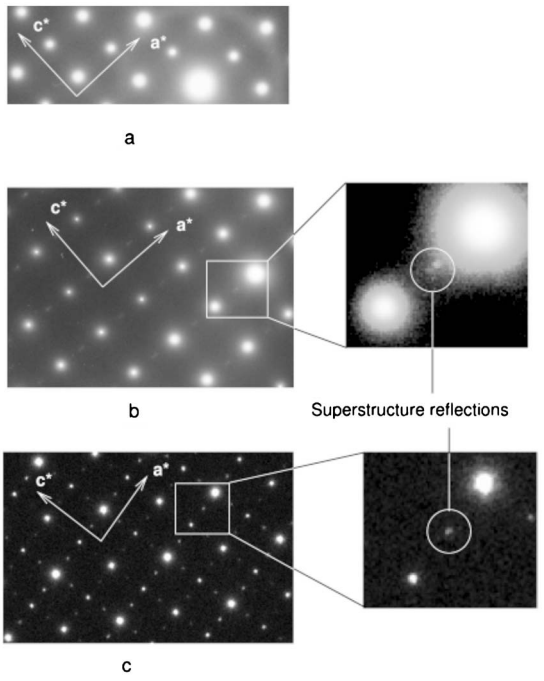

FIG. 1. Diffraction patterns for $La_{0.50}Ca_{0.50}MnO_3$ thin film on $NdGaO_3$ and $SrTiO_3$: (a) a room-temperature diffraction pattern (for a film on $NdGaO_3$) in which no superstructure reflections appear, and (b) a diffraction pattern for a film on $NdGaO_3$ taken at 90 K in which the superstructure reflections are clearly visible. (c) A diffraction pattern taken at 90 K from a thin film grown on $SrTiO_3$.

III. EXPERIMENTAL RESULTS

A. $La_{0.50}Ca_{0.50}MnO_3$ thin films

The films grown on $NdGaO_3$ gave a uniaxial superstructure, i.e., at 90 K the superstructure reflections appear along only one axis [see Fig. 1(b)]. The strength of the magnetization and of the superstructure reflections were monitored for different film thicknesses (see Fig. 2). The magnetization increased with decreasing temperature in all samples, as has previously been observed.[19] It can be seen that the magnetization at low temperatures decreases in amplitude with increasing film thickness (from $0.5\mu_B$/Mn ion at 44 nm to $0.2\mu_B$/Mn ion at 80 nm to $0.1\mu_B$/Mn ion at 123 nm). In addition, the temperature at which magnetic hysteresis appears decreases from 250 K in the 44 nm-thick film to 175 K in the 80-nm-thick film, while no hysteresis appears in the 123-nm-thick film. However, the superstructure is strongest and most distinct for the 44-nm-thick film, being much fainter in the 80-nm-thick film and not detectable in the 123-nm-thick film. Thus both the superstructure and the magnetization become stronger with decreasing film thickness. This has two implications. First, since the strain would be expected to decrease with increasing film thickness, it suggests that decreasing the level of strain in the film suppresses the superstructure, and that in fact in the absence of any strain, the superstructure cannot exist. Second, it suggests that rather than being in competition, the FM and stripe phases coexist; if the stripe phase is destroyed, a FM phase is not formed, but rather a paramagnetic insulator (PMI). This

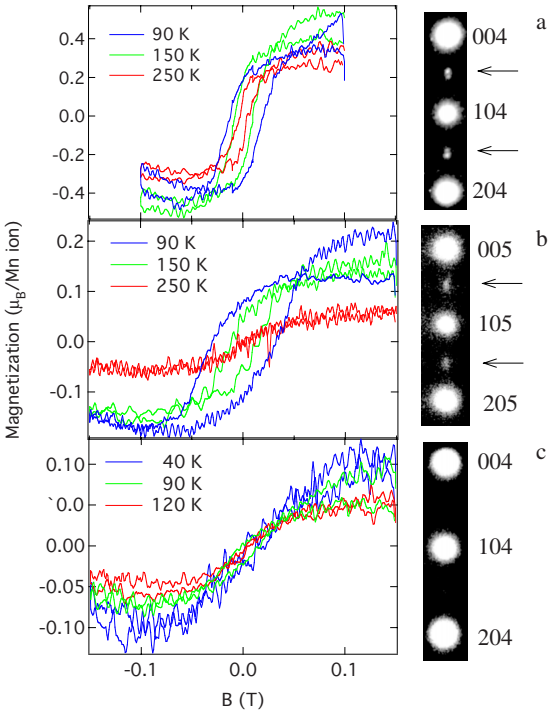

FIG. 2. (Color online) *M-H* loops at various temperatures for $La_{0.50}Ca_{0.50}MnO_3$ thin films of (a) 44 nm, (b) 80 nm, and (c) 123 nm thickness on $NdGaO_3$. The diffraction patterns at 90 K for each film are also displayed, with the superstructure reflections being visible for (a) and (b). The three diffraction patterns have been enhanced to the same degree by high-pass filtering and saturation.

is supported by a recent work, which has found that for thin films there is an area of the phase diagram ($x>0.42$, limited by the maximum x of 0.45 measured) for which the low-temperature phase is a PMI, i.e., there are no signs of the FM or stripe phases.[20] In addition, this result strongly suggests that the oxygen stoichiometry is unlikely to be driving the variations of the wave vector seen in thin films, since in this case all the films were grown on the same substrate under the same conditions, and therefore would be expected to have the same oxygen stoichiometry.

In contrast with films grown on $NdGaO_3$, films grown on $SrTiO_3$ gave diffraction patterns in which superstructure reflections appeared along both axes (see Fig. 1). By taking dark field images using superstructure reflections from each of the two directions (see Fig. 3), it was shown that the two superstructure orientations did not coexist. Instead, the images revealed small complementary regions of the different ordering orientations for the superstructure. The region of each twin extends over a length scale of 50–100 nm. The twinning occurs for films grown on $SrTiO_3$ but not on $NdGaO_3$ because of the different symmetries of the substrate: $NdGaO_3$ has an orthorhombic structure, as does $La_{0.50}Ca_{0.50}MnO_3$, and so it is always most favorable for the **a** axis of $La_{0.50}Ca_{0.50}MnO_3$ to align with the **a** axis of $NdGaO_3$. However, $SrTiO_3$ is cubic, and thus it is equally favorable for the **a** axis of $La_{0.50}Ca_{0.50}MnO_3$ to align along either the **a** or **c** axis of $SrTiO_3$.

A further difference between the properties of the $La_{0.50}Ca_{0.50}MnO_3$ superstructure in the two types of films

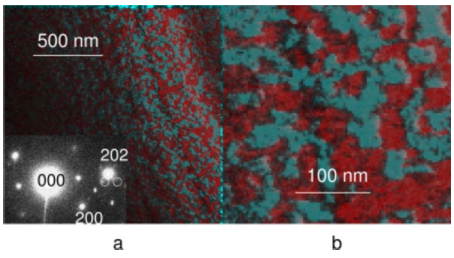

FIG. 3. (Color online) Twins of two different orientations of the low-temperature superstructure are imaged by taking two dark-field images, one from each of the circled reflections in the diffraction pattern shown as the inset of (a), and superimposing them. (As before, only one of the twins has been indexed.) One dark-field image has been tinted red (dark gray) and the other turquoise (light gray), and the lack of overlap between the two colors indicates that the two superstructure orientations do not coexist. The structure of the regions can be seen more clearly in (b).

was the value of the wave vector. Diffraction patterns of a large area were taken using a selected area aperture of 500 nm diameter, as measured in the sample plane. The selected area diffraction patterns were analyzed using software which measured the position of many superstructure reflections in one pattern.[21] The film on $NdGaO_3$ had a wave vector of $q/a^*=0.475$ in regions away from the edges, whereas the film grown on $SrTiO_3$ had a wave vector of $q/a^*=0.50$.

B. TEM measurements of $Pr_{0.48}Ca_{0.52}MnO_3$

We now turn to the TEM measurements of $Pr_{0.48}Ca_{0.52}MnO_3$. Selected area diffraction patterns were taken using an aperture of 500 nm diameter, as described above. The size of the aperture was much smaller than the grain size (2 μm).[7] Therefore the diffraction patterns measure intrinsic properties of the grains, including strain. In all patterns **q** was found to be essentially parallel to $\mathbf{a}^*$. Three diffraction patterns [Figs. 4(a)–4(c)] have values of q/a^* between 0.445 and 0.450, and the fourth shows $q/a^*=0.5$ [Fig. 4(d)]. Therefore in $Pr_{0.48}Ca_{0.52}MnO_3$ the superstructure will lock into the lattice under certain conditions, supporting the idea that the electron-lattice coupling is stronger in this compound than in $La_{0.48}Ca_{0.52}MnO_3$.

The measurements of the wave vector in the grains in which no lock-in occurred are within the range one would expect from previous measurements of $La_{0.48}Ca_{0.52}MnO_3$. It should be noted that the nominal value of $q/a^*=1-x$ is never actually observed; in fact, $q/a^*<1-x$. This deviation and the variation of the wave vector from grain to grain are traditionally ascribed to different levels of strain in the grains. This can be described in the context of a Ginzberg-Landau theory[6,22] (see Fig. 5).

Convergent-beam electron-diffraction patterns were obtained using a converged beam with a full width at half maximum of 3.6 nm, which corresponds to 6.7 room temperature unit cells in $Pr_{0.48}Ca_{0.52}MnO_3$. From the composition $x=0.52$ in a one-dimensional model of charge order using Mn^{3+} and Mn^{4+}, one would expect alternating Mn^{3+} and Mn^{4+}, with an extra Mn^{4+} every 13.6 unit cells on average.[7] This would lead to a value of $q/a^*=0.5$ being recorded in

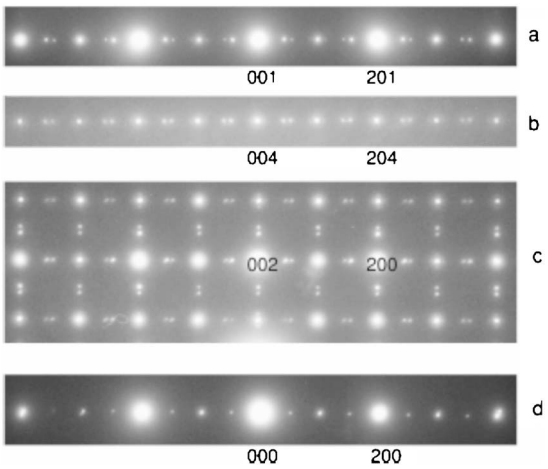

FIG. 4. Selected area-diffraction patterns taken with a 500-nm aperture from different grains of the $Pr_{0.48}Ca_{0.52}MnO_3$ sample. Pattern (c) shows twinning. Patterns (a), (b), and (c) show wave vectors with q/a^* between 0.445 and 0.45, whereas pattern (d) shows $q/a^*=0.5$.

most measurements. However, the convergent-beam electron-diffraction patterns clearly showed a periodicity equivalent within the error of the one extracted from the corresponding selected area diffraction pattern (Fig. 6). Thus the periodicity of the superstructure is uniform down to the level of a few unit cells in $Pr_{0.48}Ca_{0.52}MnO_3$.

IV. DISCUSSION

As has been previously shown,[8] the free energy of the superstructure in a Ginzberg-Landau theory is given by

$$F=\frac{\xi^2}{2}(\nabla\phi-\delta)^2+\frac{v}{n}\cos(n\phi)+c\eta\nabla\phi+\frac{1}{2}\kappa\eta^2-\sigma\eta, \tag{1}$$

where the first term is the elastic term that favors incommensurate modulation, and δ is the deviation of q/a^* in the absence of strain coupling. The second term is the umklapp term that favors commensurability, where n is the commensurability and v determines the strength of the effect. In this case $n=4$ since the periodicity of the low-temperature superstructure is four times the room-temperature pseudocubic cell.[11] The third term couples η and $\nabla\phi$ with strength c, the fourth term is the strain energy density in terms of the bulk elastic modulus κ, and the fifth term gives the elastic energy due to the stress σ on the film from the substrate. For ease of reference, these parameters are defined in Table II, which also summarizes the values obtained in the experiments described in this paper.

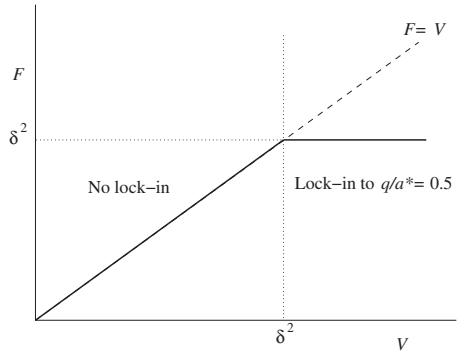

FIG. 5. Demonstrates the relations between V and F, which lead to a lock-in for $V<\delta^2$ and to no lock-in for $V>\delta^2$.

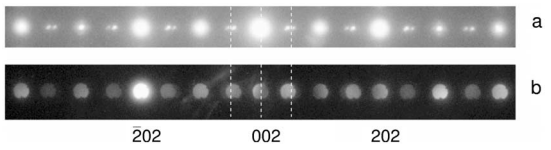

FIG. 6. (a) Selected area-diffraction and (b) convergent-beam electron-diffraction patterns from the same region of a $Pr_{0.48}Ca_{0.52}MnO_3$ grain. The wave vectors are the same within experimental error. The dotted line is at $q/a^*=0.5$.

Minimizing F in the plane-wave limit ($\nabla\phi$=constant and $\nabla\eta=0$), we find

$$\nabla\phi=\frac{\delta-\dfrac{c\sigma}{\kappa\xi^2}}{1-\dfrac{c^2}{\kappa\xi^2}}. \tag{2}$$

To calculate the approximate levels of stress in each film, the strain in the a and c directions must first be found. Let $SrTiO_3$ be substrate 1 and $NdGaO_3$ be substrate 2. Calculating the strain using the mismatch of the a and c lattice parameters for the substrate and $La_{0.50}Ca_{0.50}MnO_3$, we obtain $\eta_{1a}=0.012$, $\eta_{1c}=0.0066$, $\eta_{2a}=-0.0048$, and $\eta_{2c}=0.0035$ (see Table I). These values can be used to calculate the level of strain in the films, using $\sigma_a=E(\eta_a+\nu\eta_c)/(1-\nu^2)$, where E is the Young's modulus of the material. Using approximate values of the bulk modulus κ (135 GPa) and shear modulus (31 GPa),[11] we obtain a Young's modulus of 86 GPa and a Poisson's ratio (ν) of 0.39, giving $\sigma_{1a}=0.00405E$ and $\sigma_{2a}=0.0172E$.

Considering the results for the film on $SrTiO_3$, with $\nabla\phi_1=0$,

$$\frac{\sigma_{1a}c}{\kappa\xi^2}=\delta. \tag{3}$$

To obtain an approximate value of δ we consider the results for polycrystalline samples, and assume that the extraneous effects which render δ finite have different values in

TABLE I. In-plane strains for $La_{0.50}Ca_{0.50}MnO_3$ on $NdGaO_3$ and $SrTiO_3$ at 90 K and 300 K. Positive numbers refer to the $La_{0.50}Ca_{0.50}MnO_3$ parameter being smaller than the substrate parameter, so the film is stretched. Data from Refs. 23–25.

	η_a at 90 K	η_c at 90 K	η_a at 300 K	η_c at 300 K
$NdGaO_3$	−0.0048	0.0035	0.0017	0.0119
$SrTiO_3$	0.0012	0.0066	0.0176	0.0157

TABLE II. Table showing the meaning and values of the parameters used and derived in this paper.

Parameter	Meaning	Value/constraint $La_{0.48}Ca_{0.52}MnO_3$	Value/constraint $Pr_{0.48}Ca_{0.52}MnO_3$	Measured or derived
η	Strain due to substrate	See Table I		Derived from substrate/lattice mismatch
ξ	Electron-electron coupling			Unknown, but see v and V below
δ	Deviation of q from $0.5a^*$ in the absence of strain from a substrate	Positive-estimated value $0.0124a^*$	Positive	Inferred from literature
δ_s	Deviation of q from $0.5a^*$ in the absence of lock-in term	$0.03a^*$–$0.77a^*$ [a]	$0.05a^*$–$0.02a^*$	Measured from polycrystalline results
c	Coupling between strain and superstructure	$c/\xi^2=-1.1$, $c/\kappa=-0.3$		Derived in this paper
v	Coupling between commensurate periodicity and superstructure	$2v/n\xi^2<0.0009$, or $v/\xi^2<0.0018$	$4\times10^{-4}<2v/n\xi^2<0.0025$, or $8\times10^{-4}<v/\xi^2<0.005$	Derived in this paper
n	Commensurability	4	4	Inferred from superstructure periodicity
σ	Stress due to substrate	$0.00405E$ on $SrTiO_3$, $0.0172E$ on $NdGaO_3$		Derived from η and E
κ	Bulk modulus	135 GPa		[b]
S	Shear modulus	31 GPa		[b]
E	Young's modulus	86 GPa		Derived from S and κ
V	$=(2v/n\xi^2)=(v/2\xi^2)$ where v/ξ^2 is the ratio between strength of electron-phonon coupling and electron-electron coupling	<0.0009	0.0004–0.0025, lower values have higher probability	Derived in this paper

[a]Reference 7.
[b]Reference 11.

the different grains, and that in the thin films these effects are around the average level that they are in the different polycrystalline grains. Therefore, $\delta=0.0124a^*$ (the average δ for observations in polycrystalline $La_{0.50}Ca_{0.50}MnO_3$ samples).

Substituting into Eq. (3) gives $c/\xi^2=-1.1$ (Table II). So surprisingly, the strain coupling term is at a similar level to the elastic term that favors an incommensurate modulation.

Now we consider the film on $NdGaO_3$; substituting the values of c/ξ^2 and $\nabla\phi_{2a}=-0.025a^*$ into Eq. (1), we find

$$\frac{c^2}{\kappa\xi^2}=1-\frac{\delta}{\nabla\phi_{2a}}\left(1-\frac{\eta_1}{\eta_2}\right). \tag{4}$$

Substituting the corresponding values gives $c/\kappa=-0.3$. So the strain energy-density term is larger than the coupling term and the elastic incommensurate term.

The Ginzberg-Landau theory was used to investigate which sets of parameters could give rise to the observed wave vector values in polycrystalline $Pr_{0.48}Ca_{0.52}MnO_3$. Since we cannot quantify the levels of strain in the different grains, we take δ_s to include the deviation from $q/a^*=0.5$, which is due to strain. Then the terms in the free energy which can vary are given by

$$F=(\nabla\phi-\delta_s)^2+V\cos(n\phi), \tag{5}$$

where $V=2v/n\xi^2=v/2\xi^2$. Here, v/ξ^2 is the ratio between the strength of the electron-phonon coupling and the electron-electron coupling. The ground state can be found by minimizing this quantity with respect to ϕ, with the boundary condition that at $\phi=0$, $\nabla\phi=\delta_s+t$, where $t\ll\delta_s$. In the limit of small t, this gives $F=V$. The free energy of this state can be calculated and compared to the energy of the lock-in state, which has $\phi=\pi/8$, $\nabla\phi=0$, and thus $F=\delta^2$. So if the energy of the lock-in state is lower, the superstructure will lock in and $q/a^*=0.5$ (see Fig. 5).

Since the wave vector does not lock into the lattice for $\delta_s=0.05$, it follows that V must be smaller than δ_s^2, since above this level a lock-in should occur. However, we know that a lock-in does occur in one grain. Therefore in that grain δ is taken to be the smallest value previously observed in a manganite with $x=0.52$, which is $\delta_s=0.02$. Therefore the lock-in provides a lower bound for V, since V must be larger than δ_s^2 in this case to allow a lock-in to occur. So $0.0025<V<0.0004$ for $Pr_{0.48}Ca_{0.52}MnO_3$ (Table II). This method can also be used to provide an upper bound for V in $La_{0.48}Ca_{0.52}MnO_3$, since no lock-in is observed when $q/a^*=0.03$, giving $V<0.0009$ (Table II).

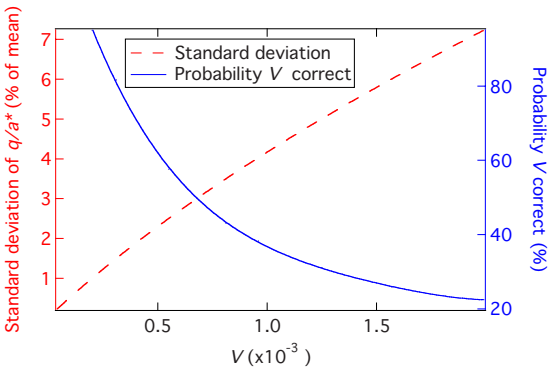

FIG. 7. (Color online) Variation of the standard deviation of q/a^* with V (red, dashed line) and the probability that a given value of V could produce the observed result (blue, solid line).

The significance of the value of the wave vector being the same at length scales of 3.6 nm and 500 nm was then investigated. The equations shown above were used to calculate the values of ϕ and $\nabla\phi$ for an array of 925 room-temperature unit cells (equivalent to the diameter of the 500 nm aperture). From this array 90 nonoverlapping regions of 6.7 unit cells were chosen. The standard deviations of the average wave vectors of these regions were found for different values of V. The results are shown in Fig. 7, displayed as a percentage of the 925-cell average. Given the 1% standard deviation in the measurement of the wave vector for the selected area diffraction and convergent-beam electron-diffraction results, we wanted to know the probability of measuring large- and small-scale values close to each other for each value of V. We assume that both the measurement of the wave vector and the simulation of the areas of 6.7 unit cells have Gaussian distributions. The probability of the convergent-beam electron-diffraction result being within 4% of the selected area-diffraction result experimentally is then 95%. Then taking the distribution of the simulation, the probability of the small-scale results being within 4% of the large-scale result can be calculated from the standard deviation at each value of V. This indicates the probability of obtaining the result we did for each value of V. As can be seen, the probability decreases with increasing V, meaning that the values of V close to 0.0004 are more likely to be correct. All parameters are summarized in Table II.

V. CONCLUSIONS

The CDW Landau theory of the manganites predicts that a lock-in should occur in the manganite superstructure when $x>0.5$, for some range of x close to 0.5. In this paper we report an observation of such a lock-in. It is also expected that the electron-phonon coupling parameter should be small relative to the electron-electron coupling parameter. Based on our data, we have used Landau theory to constrain the value of the electron-phonon coupling relative to the electron-electron coupling to between 0.08% and 0.50%, with the results indicating that the lower end of this scale has a higher probability. In addition, we have found that the coupling of the strain to the superstructure in the stripe phase is of the same magnitude as the electron-electron coupling, indicating that the coupling of the superstructure to strain is unexpectedly strong. This is particularly interesting since our results also suggest that the stripe phase cannot exist in the absence of strain. Therefore the properties of the manganite CDW can now be quantified to a reasonable extent (Table II). Our results also raise the possibility of using strain to manipulate the CDW, via the strong coupling of strain to the CDW and the possibility of destroying the CDW by releasing the strain.

ACKNOWLEDGMENTS

We thank P. B. Littlewood for helpful comments. This work is supported by U.S. DOE Grant No. LDRD-DR 20070013 and by the EPSRC. Work at the NHMFL is performed under the auspices of the NSF, DOE, and the State of Florida. Work at Cambridge was funded by the UK EPSRC and the Royal Society. S.C. acknowledges support from the Seaborg Institute.

[1] N. D. Mathur and P. B. Littlewood, Phys. Today **56**(1), 25 (2003).
[2] N. D. Mathur and P. B. Littlewood, Solid State Commun. **119**, 271 (2001).
[3] C. H. Chen, S.-W. Cheong, and H. Y. Hwang, J. Appl. Phys. **81**, 4326 (1997).
[4] J. P. Goodenough, Phys. Rev. **100**, 564 (1955).
[5] S. Cox, J. Singleton, R. D. McDonald, A. Migliori, and P. B. Littlewood, Nat. Mater. **7**, 25 (2008).
[6] G. C. Milward, M. J. Calderón, and P. B. Littlewood, Nature (London) **433**, 607 (2005).
[7] J. C. Loudon, S. Cox, N. D. Mathur, and P. A. Midgley, Philos. Mag. **85**, 999 (2005).
[8] S. Cox, E. Rosten, J. C. Chapman, S. Kos, M. J. Calderon, D. J. Kang, P. B. Littlewood, P. A. Midgley, and N. D. Mathur, Phys. Rev. B **73**, 132401 (2006).
[9] W. Prellier, A. M. Haghiri-Gosnet, B. Mercey, Ph. Lecoeur, M. Hervieu, Ch. Simon, and B. Raveau, Appl. Phys. Lett. **77**, 1023 (2000).
[10] A. Barnabé, M. Hervieu, C. Martin, A. Maignan, and B. Raveau, J. Appl. Phys. **84**, 5506 (1998).
[11] M. J. Calderón, A. J. Millis, and K. H. Ahn, Phys. Rev. B **68**, 100401(R) (2003).
[12] K. H. Ahn, T. Lookman, and A. R. Bishop, Nature (London) **428**, 401 (2004).
[13] C. H. Chen and S-W. Cheong, Phys. Rev. Lett. **76**, 4042 (1996).
[14] Z. Jirak, S. Krupixka, Z. Simsa, M. Dloha, and S. Vratislav, J. Magn. Magn. Mater. **53**, 153 (1985).
[15] J. P. Hill *et al.*, Appl. Phys. A: Mater. Sci. Process. **73**, 723 (2001).

[16] S.-W. Cheong and H. Y. Hwang, in *Colossal Magnetoresistive Oxides*, edited by Y. Tokura (Gordon and Breach, New York, 2000), pp. 237–280.
[17] S. Cox, J. C. Lashley, E. Rosten, J. Singleton, A. J. Williams, and P. B. Littlewood, J. Phys.: Condens. Matter **19**, 192201 (2007).
[18] A. J. Williams, B. M. Sobotka, and J. P. Attfield, J. Solid State Chem. **173**, 456 (2003).
[19] Y. M. Xiong, G. Y. Wang, X. G. Luo, C. H. Wang, X. H. Chen, X. Chen, and C. L. Chen, J. Appl. Phys. **97**, 083909 (2005).
[20] D. Sánchez, L. E. Hueso, L. Granja, P. Levy, and N. D. Mathur, Appl. Phys. Lett. **89**, 142509 (2006).
[21] E. Rosten and S. Cox, Lect. Notes Comput. Sci. **4291**, 373 (2006).
[22] P. Bak and J. Timonen, J. Phys. C **11**, 4901 (1978).
[23] P. G. Radaelli, D. E. Cox, M. Marezio, and S. W. Cheong, Phys. Rev. B **55**, 3015 (1997).
[24] D. Savytskii, L. Vasylechko, A. Senyshyn, A. Matkovskii, C. Bahtz, M. L. Sanjuan, U. Bismayer, and M. Berkowski, Phys. Rev. B **68**, 024101 (2003).
[25] N. V. Krainyukova and V. V. Butokii, Appl. Surf. Sci. **235**, 43 (2004).